AMERICAN SOCIETY FOR MICROBIOLOGY | Infection and Immunity

Affinity-Based Screening of Tetravalent Peptides Identifies Subtype-Selective Neutralizers of Shiga Toxin 2d, a Highly Virulent Subtype, by Targeting a Unique Amino Acid Involved in Its Receptor Recognition

Takaaki Mitsui,[a] Miho Watanabe-Takahashi,[a] Eiko Shimizu,[a] Baihao Zhang,[a] Satoru Funamoto,[b] Shinji Yamasaki,[c] Kiyotaka Nishikawa[a]

Departments of Molecular Life Sciences[a] and Neuropathology,[b] Graduate School of Life and Medical Sciences, Doshisha University, Kyoto, Japan; International Prevention of Epidemics, Graduate School of Life and Environmental Sciences, Osaka Prefecture University, Osaka, Japan[c]

Shiga toxin (Stx), a major virulence factor of enterohemorrhagic *Escherichia coli* (EHEC), can be classified into two subgroups, Stx1 and Stx2, each consisting of various closely related subtypes. Stx2 subtypes Stx2a and Stx2d are highly virulent and linked with serious human disorders, such as acute encephalopathy and hemolytic-uremic syndrome. Through affinity-based screening of a tetravalent peptide library, we previously developed peptide neutralizers of Stx2a in which the structure was optimized to bind to the B-subunit pentamer. In this study, we identified Stx2d-selective neutralizers by targeting Asn16 of the B subunit, an amino acid unique to Stx2d that plays an essential role in receptor binding. We synthesized a series of tetravalent peptides on a cellulose membrane in which the core structure was exactly the same as that of peptides in the tetravalent library. A total of nine candidate motifs were selected to synthesize tetravalent forms of the peptides by screening two series of the tetravalent peptides. Five of the tetravalent peptides effectively inhibited the cytotoxicity of Stx2a and Stx2d, and notably, two of the peptides selectively inhibited Stx2d. These two tetravalent peptides bound to the Stx2d B subunit with high affinity dependent on Asn16. The mechanism of binding to the Stx2d B subunit differed from that of binding to Stx2a in that the peptides covered a relatively wide region of the receptor-binding surface. Thus, this highly optimized screening technique enables the development of subtype-selective neutralizers, which may lead to more sophisticated treatments of infections by Stx-producing EHEC.

Shiga toxin (Stx) is a major virulence factor of enterohemorrhagic *Escherichia coli* (EHEC), which causes bloody diarrhea, hemorrhagic colitis, and sometimes life-threatening systemic complications such as acute encephalopathy and hemolytic-uremic syndrome (HUS) (1–6). To date, numerous EHEC strains that produce various Stx subtypes have been reported (7, 8). These Stxs can be classified into two subgroups, Stx1 and Stx2, each consisting of various closely related subtypes, such as Stx1a, -1c, and -1d and Stx2a, -2b, -2c, -2d, -2e, -2f, and -2g (7–9). Stx2a (10, 11) and Stx2d, which is activated by elastase derived from the intestinal mucosa (12–14), are highly virulent and have been linked with HUS, the most serious sequela of EHEC infection. The pathophysiologic importance of these subtypes was also confirmed by the finding that Stx2a and Stx2d are highly toxic when injected into mice (15, 16) or primates (17–19). Therefore, Stx neutralizers, particularly those customized to specifically neutralize Stx2a and Stx2d, would be highly valuable therapeutic agents for treating infections caused by various EHEC strains.

Stx molecules consist of a catalytic A subunit, which has RNA *N*-glycosidase activity and inhibits eukaryotic protein synthesis (20, 21), and a B-subunit pentamer. The B-subunit pentamer is responsible for high-affinity binding to the functional cell surface receptor Gb3 (Galα[1-4]-Galβ[1-4]-Glcβ-ceramide) (4, 22, 23) or Gb4 (GalNAcβ[1-3]-Galα[1-4]-Galβ[1-4]-Glcβ-ceramide), which is the receptor preferred by Stx2e (24). Each B subunit has three distinct binding sites for the trisaccharide moiety of Gb3 (i.e., sites 1, 2, and 3) (25, 26), enabling a multivalent interaction between the B-subunit pentamer and Gb3. This type of interaction contributes to the highly selective and potent binding of Stx to target cells, sometimes referred to as the "clustering effect." Accordingly, several compounds with clustered trisaccharides that can bind to the B subunit with high affinity have been developed and shown to effectively neutralize Stx both *in vitro* and *in vivo* (27–33). These compounds, however, cannot be customized to specific Stx subtypes, because all Stx subtypes recognize the trisaccharide as the natural binding unit.

Previously, we developed a library of multivalent peptides exhibiting the clustering effect, from which we identified Stx-neutralizing tetravalent peptides by screening the library for high-affinity binding to the specific receptor-binding sites (33–36). By targeting Stx2a receptor-binding site 3 or Stx1a site 1, we identified various tetravalent peptides demonstrating remarkable therapeutic potency in both a mouse model of EHEC infection (34, 36) and a nonhuman primate model (19). Recently, we established a novel technique to determine a wide range of binding

Received 22 February 2016 **Returned for modification** 11 April 2016
Accepted 24 June 2016

Accepted manuscript posted online 5 July 2016

Citation Mitsui T, Watanabe-Takahashi M, Shimizu E, Zhang B, Funamoto S, Yamasaki S, Nishikawa K. 2016. Affinity-based screening of tetravalent peptides identifies subtype-selective neutralizers of Shiga toxin 2d, a highly virulent subtype, by targeting a unique amino acid involved in its receptor recognition. Infect Immun 84:2653–2661. doi:10.1128/IAI.00149-16.

Editor: B. A. McCormick, The University of Massachusetts Medical School

Address correspondence to Kiyotaka Nishikawa, knishika@mail.doshisha.ac.jp.

motifs for the B subunit by directly screening hundreds of divalent peptides synthesized on a cellulose membrane. The amino acid sequences of these peptides were designed on the basis of information obtained from the multivalent peptide library (37). By targeting Stx1a receptor-binding site 2 of the B subunit, we identified 11 peptides that neutralize Stx1a (37). Thus, the combination of library screening and synthesis of peptides on a cellulose membrane enables the efficient design of customized neutralizing peptides targeting a specific region of the receptor-binding surface of the Stx B subunit.

The amino acid sequence of the Stx2d B subunit is highly homologous to that of the Stx2a B subunit, with a difference of only two amino acids (38), Asn16 and Ala24 of the Stx2d B subunit, corresponding to Asp16 and Asp24 of the Stx2a B subunit, respectively. Asp16 of the Stx2a B subunit constitutes functional receptor-binding site 1 (26, 32, 39). Although Asn16 of the Stx2d B subunit is predicted to form receptor-binding site 1, thus contributing to cytotoxic activity (16, 40), it is unclear whether Asn16 is directly involved in receptor binding.

Using a series of B-subunit receptor-binding site mutant forms, in the present study, we found that Asn16 of the Stx2d B subunit plays an essential role in receptor binding. We targeted Asn16 and screened a series of tetravalent peptides synthesized on a cellulose membrane, the sequences of which contained the B-subunit consensus binding motif (34, 36, 37). Using this approach, we identified two peptides that selectively neutralize Stx2d. We also investigated the molecular mechanism underlying the Stx2d-specific inhibitory effects of these neutralizing peptides.

MATERIALS AND METHODS

Materials. Gb3 polymer 1:0, which is a linear polymer of acrylamide with highly clustered trisaccharides, was obtained as described previously (31). AlphaScreen reagent and Amino-PEG_{500}-UC540 membranes (INTAVIS; Bioanalytical Instruments AG, Tübingen, Germany) used in the spot synthesis of peptides were purchased from PerkinElmer (Tokyo, Japan). Recombinant Stx2a, the histidine-tagged Stx2a B subunit (2aBH), and 2aBHs containing amino acid substitutions (2aBH-D16A, 2aBH-W29A, 2aBH-W33A, 2aBH-G61A, and 2aBH-W29A/G61A/W33A) were prepared as described previously (32). Stx2d was prepared from the culture supernatant of *E. coli* strain B2F1 (O91:H21) as described previously (41). The histidine-tagged Stx2d B subunit (2dBH) was prepared as follows. An NcoI-BamHI fragment was prepared from a lysate of *E. coli* strain B2F1 (O91:H21) by PCR with primers 5′-AGAGCCATGGATTGTGCTAAAG GTAAAATT-3′ and 5′-AGAGGGATCCGCGTCATTATTAAACTG-3′. The fragment was ligated into the vector pET-28a (Novagen, Merck, Germany). 2dBH was expressed in competent *E. coli* BL21DE (3) cells (Novagen) transformed with the vector, as described previously (31). To prepare 2dBHs containing amino acid substitutions (2dBH-N16A, 2dBH-W29A, 2dBH-G61A, 2dBH-W33A, and 2dBH-N16A/G61A/W33A), site-directed mutagenesis of pET28a-2dBH was performed with a QuikChange kit (Stratagene, CA, USA) with the following mutagenic oligonucleotides: 5′-TTTTACTGTGAATGTATCAGCCTCATTATACT TGGAAAA-3′ for N16A, 5′-CAGATTCCAGCGACTGGTAGCGTACT CTTTTCCGGCCAC-3′ for W29A, 5′-AAACTGCACTTCAGCAAAAG CGGA GCCTGATTCACAGGT-3′ for G61A, and 5′-CAGTAACGGTTG CAGATTAGCGCGACTGGTCCAGTACTC-3′ for W33A.

Kinetic analysis of binding between the Gb3 polymer and B subunits. Binding of the Gb3 polymer to 2dBH or 2dBH containing an amino acid substitution was quantified with a Biacore T100 system (GE Healthcare Sciences, USA) as described previously (34). After Ni^{2+} was fixed on a nitrilotriacetic acidic sensor chip (GE Healthcare Sciences), recombinant 2dBH or 2dBH with an amino acid substitution (10 μg/ml) was injected into the system and immobilized on the chip. Various concentrations of the Gb3 polymer were injected to reach a plateau at 25°C. Resonance was expressed in the arbitrary units (AU) used by the Biacore system. Binding kinetics were analyzed with BIAEVALUATION v1.1.1 (GE Healthcare Sciences).

Spot synthesis of tetravalent peptides on a cellulose membrane. Basic spot synthesis of peptides on a cellulose membrane was performed as described previously (37), with a ResPep SL SPOT synthesizer (INTAVIS Bioanalytical Instruments AG). Fmoc-βAla-OH (Watanabe Chemical Industries, Japan) was used in the first cycle, followed by aminohexanoic acid as a spacer. Fmoc-Lys(Fmoc)-OH (Watanabe Chemical Industries) was used in the next two cycles to create four branches in the peptide chain for subsequent motif synthesis. Prior to deprotection of the side chain residues, successful synthesis of each peptide was confirmed by staining the membrane with bromophenol blue (1% in *N*,*N*′-dimethylformamide), which reacts with the free amino residues produced only after completion of all of the reactions. After destaining with *N*,*N*′-dimethylformamide, the membrane was used in the binding assay.

Assay of 2dBH or 2dBH-N16A binding to tetravalent peptides. After blocking with 5% skim milk in phosphate-buffered saline, the membrane, prepared as described above, was blotted for 1 h at room temperature with ^{125}I-labeled 2dBH or ^{125}I-labeled 2dBH-N16A (1 μg/ml, 1×10^6 to 2×10^6 cpm/μg of protein) prepared as described previously (34). After extensive washing, the radioactivity bound to each peptide spot was quantified in terms of the number of pixels with a BAS 2500 bioimaging analyzer (GE Healthcare, Japan) as described previously (37).

Synthesis of tetravalent peptides. Tetravalent peptides were synthesized with *N*-α-9-fluorenylmethoxy carbonyl (Fmoc)-protected amino acids and standard (benzotriazol-1-yloxy)tris(dimethylamino)phosphonium hexafluorophosphate/1-hydroxybenzotriazole hydrate coupling chemistry as described previously (34). A Met-Ala sequence was included at the amino terminus of the tetravalent peptide so that its structure would be identical to that of MMA-tet, which was developed on the basis of the results of multivalent peptide library screening and found to effectively inhibit both Stx1a and Stx2a (36). The terminal amino groups of the tetravalent peptides were biotinylated with biotin (Sigma-Aldrich, USA) and 1-(bis[dimethylamino]methylene)-1*H*-benzotriazolium 3-oxide hexafluorophosphate (Peptide Institute Inc., Japan) in the last cycle of the peptide synthesis.

Cytotoxicity assay. Subconfluent Vero cells cultured in a 96-well plate in Dulbecco's modified Eagle's medium supplemented with 10% fetal calf serum were treated with Stx2a (10 pg/ml) or Stx2d (80 pg/ml) in the absence or presence of a given tetravalent peptide for 72 h at 37°C. The relative number of living cells remaining after treatment was determined with Cell Counting Kit-8 (Dojindo, Japan) as described previously (34).

Analysis of binding between tetravalent peptides and B subunits with the AlphaScreen assay. The AlphaScreen assay was used to assess binding between the tetravalent peptides and Stx B subunits as described previously (36). Various amounts of biotinylated tetravalent peptide and mutant 2aBH, 2dBH, or 2aBH/2dBH (10 μg/ml) were incubated in individual wells of an OptiPlate-384 (PerkinElmer) for 1 h at room temperature. The samples were then incubated with nickel chelate acceptor beads (20 μg/ml; PerkinElmer) for 30 min and then with streptavidin donor beads (20 μg/ml; PerkinElmer) for 1 h at room temperature in the dark. The plate was then subjected to excitation at 680 nm, and emission from the wells was monitored at 615 nm with an EnVision system (PerkinElmer). Data are expressed as the AU of signal intensity (counts per second) used by the EnVision system. The apparent K_D value for each tetravalent peptide was determined as the concentration yielding half of the maximum binding value.

RESULTS

Asn16 of the Stx2d B subunit plays an essential role in receptor binding. There is a difference of two amino acids between the sequences of the Stx2a B subunit and the Stx2d B subunit. Asn16, but not Ala24, of the Stx2d B subunit is located on the receptor-

TABLE 1 Kinetic analysis of Gb3 polymer 1:0 binding to a series of Stx2d B-subunit mutant forms[a]

Stx2d B subunit	Mutated site	Mean K_D (μM) ± SE	Mean RU_{max} ± SE (*n*)
2dBH		0.32 ± 0.03	438 ± 69.3 (8)
2dBH-N16A	1	58.7 ± 33[b]	19.6 ± 6.4[c] (3)
2dBH-W29A	1	34.5 ± 7.1	53.1 ± 2.4[d] (3)
2dBH-G61A	2	1.53 ± 0.05	246 ± 18.6 (3)
2dBH-W33A	3	16.5 ± 5.3	60.8 ± 13.3[d] (3)

[a] The kinetics of Gb3 polymer 1:0 binding to each immobilized Stx2d B-subunit mutant form were analyzed with the Biacore system. RU_{max}, maximum resonance unit. The concentration of Gb3 polymer 1:0 is shown as the trisaccharide moiety. The resonance unit is an AU used by the Biacore system.
[b] $P = 0.027$ (compared with 2dBH by ANOVA and Scheffe's test).
[c] $P < 0.01$ (compared with 2dBH by ANOVA and Scheffe's test).
[d] $P < 0.02$ (compared with 2dBH by ANOVA and Scheffe's test).

binding surface (38). Although Asn16 is predicted to form receptor-binding site 1 (16, 40), there is no direct evidence demonstrating that Asn16 is involved in Stx2d receptor binding. To elucidate the role of this residue in receptor binding, Asn16 was substituted with an Ala residue and the effect on receptor-binding activity was examined with Gb3 polymer 1:0, a linear polymer of acrylamide with highly clustered trisaccharides that functions as an excellent receptor mimic (31). The effects of Ala substitutions for other amino acids (i.e., Trp29, Gly61, and Trp33, which are predicted to form sites 1, 2, and 3, respectively) were also examined. Among the 2dBH mutant forms, the K_D values for binding to 2dBH-N16A, -W29A, and -W33A increased 183-, 108-, and 52-fold, respectively, whereas the K_D value for binding to 2dBH-G61A increased only slightly, by 4.8-fold (Table 1). The maximum binding (RU_{max}) values for 2dBH-N16A, -W29A, -G61A, and -W33A decreased to 4, 12, 56, and 14% of that for 2dBH, respectively. These results indicate that Asn16 contributes significantly to the receptor binding of 2dBH and suggest that Asn16 represents an ideal target for identifying Stx2d-selective neutralizers.

Screening of tetravalent peptides synthesized on a membrane to identify peptide motifs that specifically bind to 2dBH via Asn16. We recently developed a single cellulose membrane-based technique to synthesize divalent peptides with increased affinity for binding to the B subunit (37). Here, we established another novel membrane-based technique with Fmoc-Lys(Fmoc)-OH to synthesize tetravalent peptides for the subsequent synthesis of various motifs (Fig. 1A). The basic structure of the tetravalent peptide was designed to be exactly the same as that of the previously developed tetravalent peptide library (34) in order to satisfy all of the structural requirements critical for fully exerting the clustering effect for B-subunit binding (32, 34).

The tetravalent peptide motif was either XMA-RRRR or MMX-RRRR (where X denotes any amino acid except Cys), based on the motif of MMA-tet (MMA-RRRR), which markedly inhibits the cytotoxicity of both Stx1a and Stx2a (36). Previous reports have demonstrated the importance of the second Met residue for high-affinity binding to the B subunit (36), as well as the importance of the clustered Arg residues as a consensus Stx B-subunit binding motif (34, 36, 37). These results provided the rationale for the design and on-membrane synthesis of the tetravalent peptides examined in the present study (Fig. 1B).

The membrane was blotted with ^{125}I-2dBH or ^{125}I-2dBH-N16A (Fig. 1B), and the radioactivity bound to each peptide spot was quantified and analyzed (Fig. 1C). The ratio (2dBH/N16A) of ^{125}I-2dBH binding (2dBH-binding value) to ^{125}I-2dBH-N16A binding (N16A-binding value) was calculated and normalized to evaluate the specificity of binding through Asn16. The product of the 2dBH-binding value and the normalized 2dBH/N16A ratio (2dBH × ratio) was used to evaluate both binding intensity and specificity. Nine sequences with 2dBH-binding values of >1.20 (i.e., KMA-, LMA-, QMA-, IMA-, RMA-, MMK-, MMV-, MMS-, and MMM-RRRR) were identified as candidate motifs for high-affinity binding. Of these sequences, the LMA-RRRR and MMM-RRRR motifs were found to have the highest 2dBH × ratio product in each group, indicating that these motifs exhibit the highest Asn16-mediated binding intensity and selectivity. All nine of the above-mentioned motifs were assembled into tetramer forms with the same core structure and designated KMA-tet, LMA-tet, QMA-tet, IMA-tet, RMA-tet, MMK-tet, MMV-tet, MMS-tet, and MMM-tet, respectively.

LMA-tet and MMM-tet selectively inhibit Stx2d cytotoxicity. The effects of the nine tetravalent peptides described in the previous section on the cytotoxicity of Stx2a and Stx2d are illustrated in Fig. 2. At a concentration as low as 17 μM, LMA-tet, QMA-tet, IMA-tet, MMV-tet, and MMM-tet inhibited the cytotoxicity of Stx2a similarly to MMA-tet (the most effective peptide-based neutralizer of this subtype developed to date) (Fig. 2A and C). Notably, LMA-tet and MMM-tet inhibited the cytotoxicity of Stx2d with even more potency than MMA-tet, whereas QMA-tet, IMA-tet, and MMV-tet showed inhibitory efficacy similar to that of MMA-tet (Fig. 2B and D). The 50% inhibitory concentrations (IC_{50}s) of LMA-tet, MMM-tet, and MMA-tet for Stx2d were 2.9, 2.7, and 6.8 μM, respectively, and their IC_{50}s for Stx2a were 7.9, 6.8, and 5.5 μM, respectively. KMA-tet, RMA-tet, and MMK-tet showed no or limited inhibition of Stx2a and Stx2d cytotoxicity (Fig. 2A to D). In the absence of toxin, no cytotoxic activity was exhibited by any of the nine tetravalent peptides at concentrations of up to 17 μM (data not shown). Thus, five peptides (LMA-tet, QMA-tet, IMA-tet, MMV-tet, and MMM-tet) were identified as novel neutralizers of both Stx2a and Stx2d. LMA-tet and MMM-tet, in particular, exhibited clear selectivity for Stx2d.

LMA-tet and MMM-tet bind to the Stx2d B subunit via a relatively large region of the receptor-binding surface encompassing Asn16. To elucidate the mechanism by which LMA-tet and MMM-tet bind to the Stx2a or Stx2d B subunit, the binding to each B subunit or its receptor-binding site mutant forms was examined with the AlphaScreen assay. The results showed that LMA-tet and MMM-tet bound to 2aBH or 2dBH with high affinity (Fig. 3A). The patterns of binding to 2aBH and its mutant forms were quite similar, in that the maximum values of binding to 2aBH-D16A (a site 1 mutant form) and 2aBH-W29A/G61A/W33A (a site 1, 2, and 3 triple mutant form) were markedly reduced. The maximum values of LMA-tet and MMM-tet binding to 2aBH-W33A (a site 3 mutant form) were reduced to 66.4 and 74.3%, respectively, and the apparent K_D values were increased 5.1- and 4.2-fold, respectively (Fig. 3B). On the other hand, the maximum values of LMA-tet binding to 2aBH-W29A (a site 1 mutant form) and 2aBH-G61A (a site 2 mutant form) were not markedly affected, although the apparent K_D values were increased 4.8- and 1.7-fold, respectively (Fig. 3B). Similarly, the maximum values of MMM-tet binding to 2aBH-W29A and 2aBH-G61A were not affected, but the apparent K_D values were increased 3.8- and 1.5-fold, respectively (Fig. 3B). These results

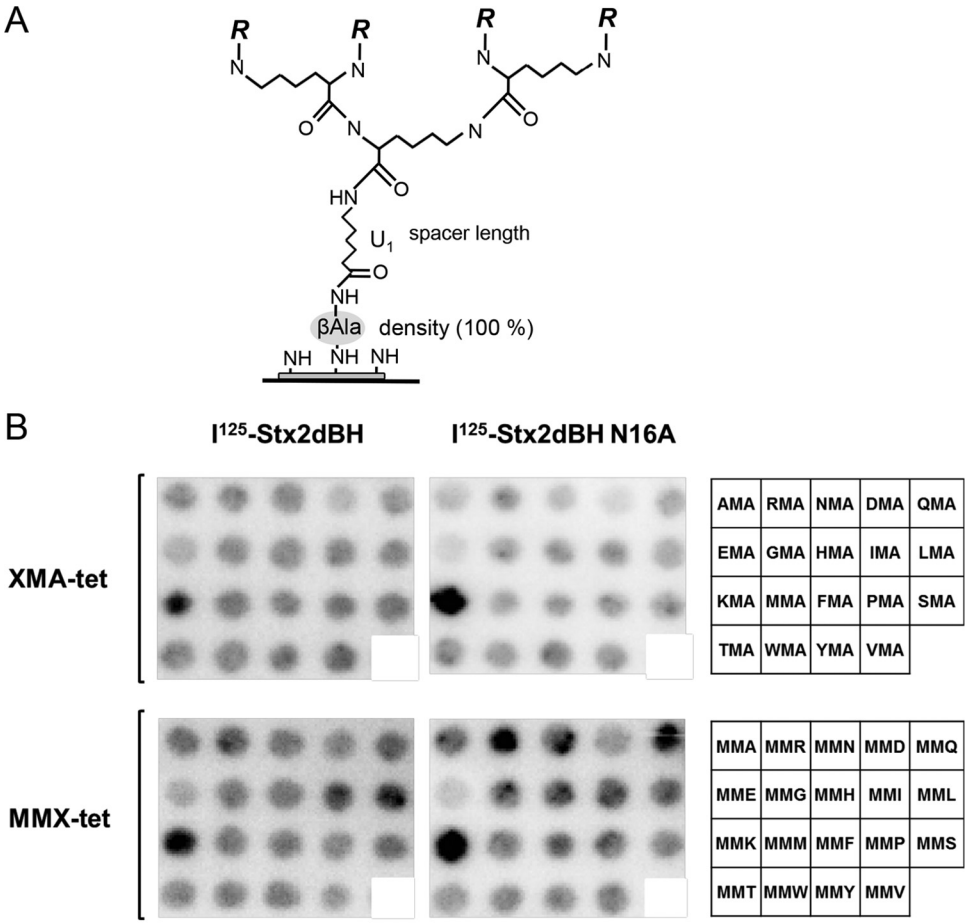

C

XMA-tet

XXX	2dBH-binding value	N16A-binding value	2dBH/N16A	2dBH X ratio
KMA	1.825	2.400	0.697	1.272
LMA	1.624	1.022	1.456	2.365
QMA	1.292	1.626	0.728	0.941
IMA	1.280	1.149	1.021	1.307
RMA	1.276	1.745	0.670	0.855
AMA	1.036	1.000	0.949	0.983
NMA	1.018	1.363	0.685	0.697
SMA	1.011	0.718	1.291	1.305
HMA	0.994	1.048	0.870	0.865
GMA	0.942	0.940	0.918	0.865
MMA	0.909	0.782	1.066	0.969
DMA	0.887	0.713	1.140	1.011
FMA	0.864	0.778	1.014	0.876
YMA	0.835	0.603	1.270	1.060
WMA	0.778	0.631	1.131	0.880
TMA	0.751	0.605	1.137	0.854
PMA	0.749	0.881	0.780	0.584
VMA	0.472	0.729	0.593	0.280
EMA	0.460	0.267	1.580	0.727

MMX-tet

XXX	2dBH-binding value	N16A-binding value	2dBH/N16A	2dBH X ratio
MMK	1.667	3.737	0.394	0.657
MMV	1.287	0.996	1.141	1.468
MMS	1.235	1.036	1.053	1.300
MMM	1.211	0.864	1.238	1.499
MMP	1.093	0.942	1.024	1.119
MMW	1.079	0.971	0.982	1.060
MMT	1.047	1.121	0.825	0.864
MMY	1.039	1.210	0.758	0.788
MMH	1.001	0.894	0.990	0.991
MMF	0.998	0.880	1.002	1.000
MMI	0.945	0.926	0.902	0.852
MMN	0.939	0.559	1.485	1.394
MMG	0.922	0.865	0.942	0.869
MML	0.919	0.845	0.961	0.883
MMA	0.871	0.667	1.154	1.005
MMR	0.854	0.914	0.825	0.705
MMQ	0.782	0.764	0.905	0.708
MME	0.637	0.463	1.215	0.774
MMD	0.472	0.347	1.204	0.568

FIG 1 Identification of Asn16-dependent 2dBH binding motifs by screening of tetravalent peptides synthesized on a cellulose membrane. (A) General structure of the tetravalent peptides synthesized on a cellulose membrane as described previously (37). The density of the tetravalent peptide was maximized by using Fmoc-β-Ala-OH without butoxycarbonyl-β-Ala-OH for the first peptide synthesis cycle. After the addition of one aminohexanoic acid (U) as a spacer following the first β-Ala, Fmoc-Lys(Fmoc)-OH was used for the next two cycles to form four branches in the peptide chain for subsequent synthesis of the various motifs examined in this study (*R* = Met-Ala-[indicated motif]-Ala-). (B) The tetravalent form of the XMA-RRRR or MMX-RRRR (X indicates any amino acid except Cys) motif was synthesized on a membrane (left and center). The first three amino acids present in the motif are indicated on the right. The membrane was blotted with ^{125}I-2dBH or ^{125}I-2dBH-N16A (1 μg/ml), and the radioactivity bound to each peptide spot was quantified as a pixel value. (C) The sum of the pixel values of all of the peptide spots was normalized to 19 (the number of tetravalent peptides synthesized on the membrane) so that each peptide would have a value of 1 in the absence of selectivity. The ratio of ^{125}I-2dBH binding (2dBH-binding value) to ^{125}I-2dBH-N16A binding (N16A-binding value) (2dBH/N16A) was calculated, and the sum of each ratio was also normalized to 19 to evaluate the specificity of binding through Asn16. The product of the 2dBH-binding value and the normalized 2dBH/N16A ratio (2dBH × ratio) was used to evaluate both binding intensity and specificity. The sequences were sorted in descending order on the basis of the 2dBH-binding values. 2dBH-binding values of >1.20 and the highest 2dBH × ratio products are shaded.

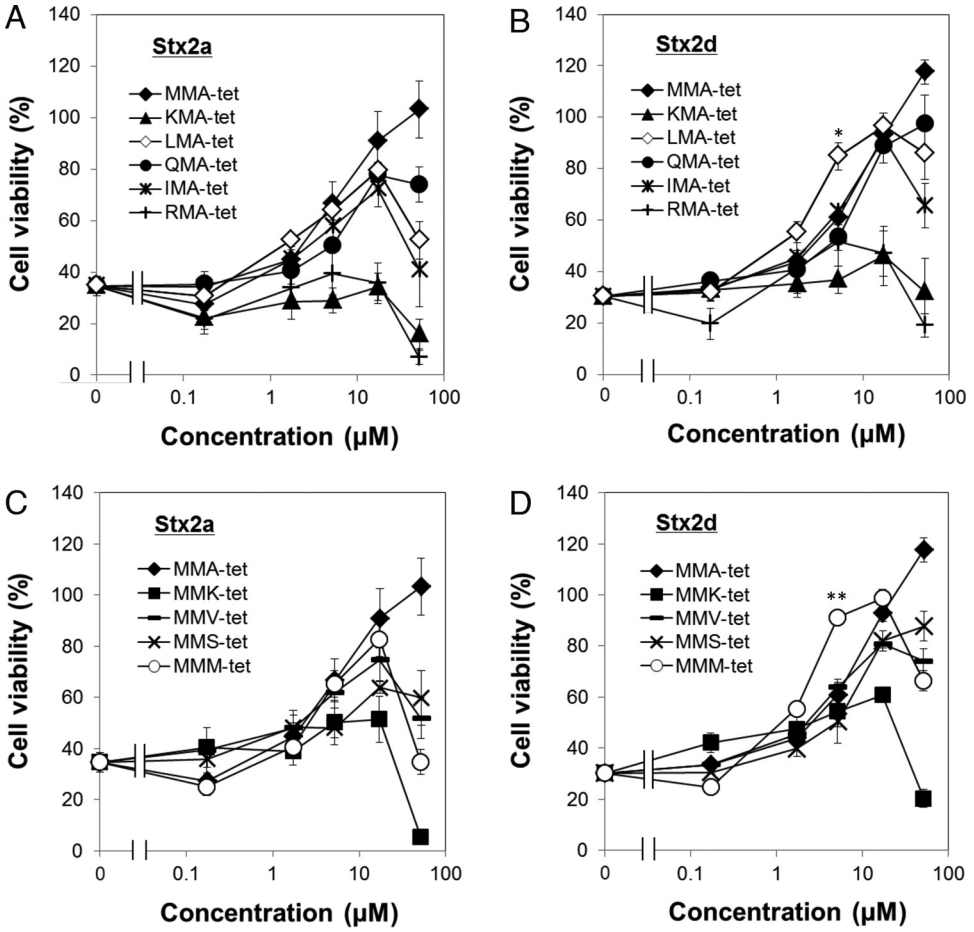

FIG 2 Inhibition of the cytotoxicity of Stx2a and Stx2d for Vero cells by the tetravalent peptides identified in this study. The effects of the tetravalent peptides indicated on the cytotoxicity of Stx2a (10 pg/ml; A and C) or Stx2d (80 pg/ml; B and D) for Vero cells were examined with a cytotoxicity assay. Data are presented as percentages of the control value (mean ± standard error, $n = 3$; *, $P < 0.05$; **, $P < 0.01$ [Tukey's test, compared with MMA-tet]).

suggest that Asp16, located at site 1 of the Stx2a B subunit, plays an essential role in the binding of LMA-tet and MMM-tet, whereas site 3 residue Trp33 (but not Trp29 at site 1 or Gly61 in site 2) plays a more limited role in binding.

In contrast, the maximum values of LMA-tet and MMM-tet binding to 2dBH-G61A (a site 2 mutant form), 2dBH-W33A (a site 3 mutant form), and 2aBH-W29A/G61A/W33A (a site 1, 2, and 3 triple mutant form) were markedly reduced, and the maximum values of binding to 2dBH-N16A (a site 1 mutant form) were substantially reduced (to 23.2 and 31.2% of the maximum binding to 2dBH, respectively) (Fig. 3B). The maximum values of LMA-tet and MMM-tet binding to 2dBH-W29A (a site 1 mutant form) were reduced to 62.1 and 57.0%, respectively, and their apparent K_D values increased 3.4- and 4.5-fold, respectively (Fig. 3B). Thus, in the case of the Stx2d B subunit, Asn16, Gly61, and Trp33, which constitute receptor-binding sites 1, 2, and 3, respectively, play significant roles in the binding of LMA-tet and MMM-tet, whereas Trp29 plays a more limited role. MA-tet, which has the same core structure as the other peptide but lacks a binding motif, did not bind to the B subunit (data not shown), providing further confirmation that the two motifs identified here mediate efficient binding to the Stx2d B subunit.

DISCUSSION

In this study, we found that Asn16 of the Stx2d B subunit, which is the only difference between the sequences of Stx2a and Stx2d on the receptor-binding surface, plays an essential role in the receptor binding of Stx2d. By Asn16-targeted screening of a series of tetravalent peptides synthesized on a cellulose membrane, we identified five novel Stx2d neutralizers: LMA-tet, QMA-tet, IMA-tet, MMV-tet, and MMM-tet. Each of these tetravalent peptides efficiently inhibited Stx2a as well. Interestingly, LMA-tet and MMM-tet exhibited clear selectivity for Stx2d.

The relative contributions of Asn16, Trp33, and Trp29 to receptor binding of the Stx2d B subunit were elucidated with Gb3 polymer 1:0, an excellent receptor mimic composed of highly clustered trisaccharides (31) (Table 1). In a previous study, we demonstrated that single substitution of Stx2a B-subunit residue Asp16, Trp29, or Trp33 with Ala has no effect on the binding kinetics of the Gb3 polymer, because in this case, the dysfunction in the corresponding receptor-binding site can be compensated for by the other sites (39). Conversely, an enzyme-linked immunosorbent assay-based study revealed that the binding of Stx2a and Stx2d B subunits to immobilized Gb3 exhibits essentially the same kinetics (42). Furthermore, the K_D value for binding of the

A

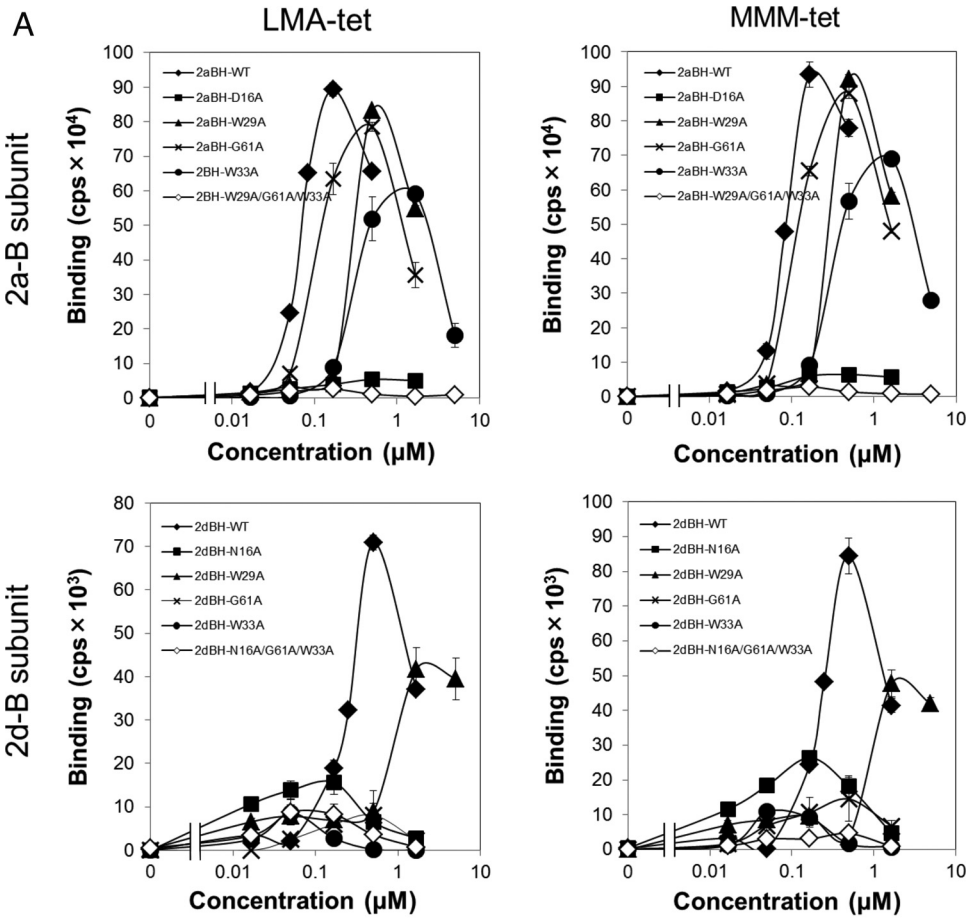

B

2BH	LMA–tet		MMM–tet	
	Apparent K_D (μM)	Maximun binding (%)	Apparent K_D (μM)	Maximun binding (%)
	mean ± se			
2aBH	0.069 ± 0.001	100	0.086 ± 0.006	100
2aBH–D16A	–	–	–	–
2aBH–W29A	0.33 ± 0.01***	93.3 ± 2.8	0.33 ± 0.01***	99.3 ± 7.7
2aBH–G61A	0.12 ± 0.01	88.1 ± 4.6	0.13 ± 0.01	95.0 ± 5.9
2aBH–W33A	0.35 ± 0.05***	66.4 ± 3.8***	0.36 ± 0.05***	74.3 ± 5.7*
2aBH–W29A/G61A/W33A	–	–	–	–
2dBH	0.28 ± 0.02	100	0.24 ± 0.02	100
2dBH–N16A	–	23.2 ± 6.0***	–	31.2 ± 1.0***
2dBH–W29A	0.96 ± 0.14**	62.1 ± 11***	1.07 ± 0.01**	57.0 ± 7.4***
2dBH–G61A	–	12.0 ± 5.9***	–	16.4 ± 9.9***
2dBH–W33A	–	12.8 ± 4.2***	–	13.2 ± 3.7***
2dBH–N16A/G61A/W33A	–	13.1 ± 6.7***	–	–

FIG 3 Analysis of the binding of LMA-tet and MMM-tet to 2aBH or 2dBH with the AlphaScreen assay. (A) The binding of biotinylated LMA-tet and MMM-tet to 2aBH, 2dBH, and their mutant forms (10 μg/ml) was examined with the AlphaScreen assay. Data are presented as signal intensity (mean number of counts per second ± standard error, $n = 3$). (B) The apparent K_D values of LMA-tet and MMM-tet for binding to 2aBH, 2dBH, and their mutant forms were determined as the concentration of the compound yielding half of the maximum binding value. The maximum values of LMA-tet and MMM-tet binding are presented as percentages of the values of their binding to 2aBH and 2dBH. —, not determined. *, $P < 0.05$; ***, $P < 0.005$ (Tukey's test); **, $P < 0.005$ (Student's t test, compared with 2aBH or 2dBH).

Gb3 polymer to the Stx2d B subunit (0.32 μM) (Table 1) was found to be even lower than that of binding to the Stx2a B subunit (0.68 μM) (39). These observations clearly indicate that the molecular interaction with the receptor differs for the Stx2a B subunit and Stx2d B subunit. Thus, Stx2d B-subunit Asn16 plays a physiologically more significant role in receptor binding than Stx2a B-subunit Asp16, further confirming the validity of selecting Asn16 as a target for the development of Stx2d-selective neutralizers.

In this study, we established a technique for cellulose membrane synthesis of tetravalent peptides with structures that satisfy all of the requirements for exerting the clustering effect for B-subunit binding (32, 34). Using a series of carbosilane dendrimers with clustered trisaccharides, referred to as SUPER TWIGs, we previously found that four trisaccharides, each of which is included in the structure separated by spacers of at least 11 Å, are sufficient for high-affinity binding to the B subunits of Stx1 and Stx2 (32). On the basis of our previous findings, our membrane peptide synthesis technique was optimized in the present study in order to synthesize tetravalent peptides containing an RRRR sequence motif. One of the four inhibitory motifs identified by targeting site 3 of the Stx2a B subunit by the peptide library technique contains a PPP-RRRR sequence (34). In addition, all of the inhibitory motifs identified by targeting site 1 (36) and site 2 (37) of the Stx1a B subunit have an RRRR motif. Replacing the RRRR motif with a DDDD motif completely abolishes binding to the Stx1a B subunit (37). In this study, screening of two series of tetravalent peptides synthesized on a membrane with XMA-RRRR or MMX-RRRR motifs led to the identification of nine candidate Stx2d B-subunit binding motifs. However, as shown in Fig. 1C, the addition of an Asp or Glu residue next to the RRRR motif yielded the lowest value of binding to the Stx2d B subunit, further confirming the importance of the cluster of basic amino acids for binding to the Stx2d B subunit.

To date, a variety of Stx neutralizers containing a cluster of trisaccharides as an Stx binding unit have been developed (27–32). However, it is difficult to develop subtype-selective neutralizers based on these neutralizers, because all of the Stx subtypes recognize Gb3 as a common receptor (4, 22–24). The B subunits of Stx2a, Stx2c, and Stx2d, in particular, display similar glycolipid-binding affinities (42). In this study, by targeting Asn16 of the Stx2d B subunit, we identified two Stx2d-selective neutralizers, LMA-tet and MMM-tet. Interestingly, Asn16, Gly61, and Trp33 of the Stx2d B subunit (which constitute receptor-binding sites 1, 2, and 3, respectively) were found to contribute equally to the efficient binding of LMA-tet and MMM-tet, whereas the corresponding Stx2a B-subunit amino acid Asp16 in site 1 (but not Gly61 or Trp33) was essential for neutralizer binding (Fig. 3). These observations clearly demonstrate that the mechanism by which the neutralizers bind to the B-subunit receptor-binding surface differs for Stx2d and Stx2a, even though both Asn16 of the Stx2d B subunit and Asp16 of the Stx2a B subunit are involved. This unique binding mechanism may contribute to the Stx2d-selective inhibitory activity of the neutralizers we identified. Of note, G61 of the Stx2d B subunit was found to be essential for the binding of LMA-tet and MMM-tet (Fig. 3), whereas this amino acid was not involved in the binding of Gb3 polymer 1:0 (Table 1), indicating that the peptide neutralizers and the Gb3 polymer bind to the Stx2d B subunit via different molecular mechanisms. Thus, the best region to target for developing a subtype-selective Stx neutralizer may not necessarily be consistent with the functional receptor-binding regions, further demonstrating the difficulty of using trisaccharides as Stx-binding units in the development of subtype-selective neutralizers.

Of the various Stx subtypes, Stx2a (10, 11) and Stx2d (12–14) are highly toxic and have been linked with HUS. Another Stx2 subtype, Stx2c, is also commonly associated with HUS (43, 44). Although Stx2c is much less toxic than Stx2a and Stx2d *in vivo* because of the instability of its A subunit (16, 45), the amino acid sequence of its B subunit is the same as that of the Stx2d B subunit (8, 43). Interestingly, we found that LMA-tet and MMM-tet also efficiently inhibited the cytotoxicity of Stx2c for Vero cells, with IC_{50}s of 2.2 and 1.6 μM, respectively, compared with 3.3 μM for MMA-tet (data not shown). As shown here, LMA-tet and MMM-tet clearly exhibited Stx2d inhibitory effects superior to those of MMA-tet (Fig. 2). MMA-tet, which was originally developed for Stx1a (36), is a universal neutralizer that efficiently inhibits various Stx subtypes, including Stx1a, Stx2a (36, 37), and Stx2d (Fig. 2). These observations clearly demonstrate the usefulness of developing subtype-selective neutralizers in addition to a universal neutralizer such as MMA-tet. LMA-tet and MMM-tet also exhibited potent inhibition of the cytotoxicity of Stx2a, with IC_{50}s (7.9 and 6.8 μM, respectively) similar to that of MMA-tet (5.5 μM) (Fig. 2). Thus, the use of these compounds alone or in combination with MMA-tet is predicted to be a more effective treatment for infections with EHEC producing these highly virulent Stx subtypes.

ACKNOWLEDGMENTS

We thank Mika Fukumoto (Doshisha University) for technical assistance.

This work was supported by a grant from the MEXT-Supported Program for the Strategic Research Foundation at Private Universities; JSPS KAKENHI grants 24390035 and 15K08480; the Research Program on Emerging and Re-emerging Infectious Diseases of the Japan Agency for Medical Research and Development, AMED; the Research Program on Development of New Drugs, AMED; the Mochida Memorial Foundation for Medical and Pharmaceutical Research; and a grant from the Asahi Glass Foundation, Japan.

FUNDING INFORMATION

This work, including the efforts of Kiyotaka Nishikawa, was funded by Japan Society for the Promotion of Science (JSPS) KAKENHI (24390035). This work, including the efforts of Miho Watanabe-Takahashi, was funded by Japan Society for the Promotion of Science (JSPS) KAKENHI (15K08480). This work, including the efforts of Kiyotaka Nishikawa, was funded by The Research Program on Emerging and Re-emerging Infectious Diseases From Japan Agency for Medical Research and Development. This work, including the efforts of Kiyotaka Nishikawa, was funded by The Research Program on Development of New Drugs From Japan Agency for Medical Research and Development. This work, including the efforts of Kiyotaka Nishikawa, was funded by Ministry of Education, Culture, Sports, Science, and Technology (MEXT) for the Strategic Research Foundation at Private Universities. This work, including the efforts of Miho Watanabe-Takahashi, was funded by The Mochida Memorial Foundation for Medical and Pharmaceutical Research. This work, including the efforts of Miho Watanabe-Takahashi, was funded by Asahi Glass Foundation, Japan.

REFERENCES

1. **Karmali MA, Steele BT, Petric M, Lim C.** 1983. Sporadic cases of hemolytic uremic syndrome associated with fecal cytotoxin and cytotoxin-producing *Escherichia coli*. Lancet **i:**619–620.
2. **Riley LW, Remis RS, Helgerson SD, McGee HB, Wells JG, Davis BR, Hebert RJ, Olcott ES, Johnson LM, Hargrett NT, Blake PA, Cohen ML.** 1983. Hemorrhagic colitis associated with a rare *Escherichia coli* serotype. N Engl J Med **308:**681–685. http://dx.doi.org/10.1056/NEJM198303243081203.
3. **O'Brien AD, Holmes RK.** 1987. Shiga and Shiga-like toxins. Microbiol Rev **51:**206–220.
4. **Paton JC, Paton AW.** 1998. Pathogenesis and diagnosis of Shiga toxin-producing *Escherichia coli* infections. Clin Microbiol Rev **11:**450–479.
5. **Tarr PI, Gordon CA, Chandler WL.** 2005. Shiga-toxin-producing Escherichia coli and haemolytic uraemic syndrome. Lancet **365:**1073–1086.
6. **Trachtman H, Austin C, Lewinski M, Stahl RA.** 2012. Renal and neu-

rological involvement in typical Shiga toxin-associated HUS. Nat Rev Nephrol **8:**658–669. http://dx.doi.org/10.1038/nrneph.2012.196.
7. **Gyles CL.** 2007. Shiga toxin-producing *Escherichia coli*: an overview. J Anim Sci **85:**E45–E62. http://dx.doi.org/10.2527/jas.2006-508.
8. **Scheutz F, Teel LD, Beutin L, Pierard Dpdote Buvens G, Karch H, Mellmann A, Caprioli A, Tozzoli R, Morabito S, Strockbine NA, Melton-Celsa AR, Sanchez M, Persson S, O'Brien AD.** 2012. Multicenter evaluation of a sequence-based protocol for subtyping Shiga toxins and standardizing Stx nomenclature. J Clin Microbiol **50:**2951–2963. http://dx.doi.org/10.1128/JCM.00860-12.
9. **Melton-Celsa AR.** 2014. Shiga toxin (Stx) classification, structure, and function. Microbiol Spectr **2:**EHEC-0024-2013.
10. **Ostroff SM, Tarr PI, Neill MA, Lewis JH, Hargrett-Bean N, Kobayashi JM.** 1989. Toxin genotypes and plasmid profiles as determinants of systemic sequelae in *Escherichia coli* O157:H7 infections. J Infect Dis **160:**994–998. http://dx.doi.org/10.1093/infdis/160.6.994.
11. **Tesh VL, Burris JA, Owens JW, Gordon VM, Wadolkowski EA, O'Brien AD, Samuel JE.** 1993. Comparison of the relative toxicities of Shiga-like toxins type I and type II for mice. Infect Immun **61:**3392–3402.
12. **Melton-Celsa AR, Darnell SC, O'Brien AD.** 1996. Activation of Shiga-like toxins by mouse and human intestinal mucus correlates with virulence of enterohemorrhagic *Escherichia coli* O91:H21 isolates in orally infected, streptomycin-treated mice. Infect Immun **64:**1569–1576.
13. **Kokai-Kun JF, Melton-Celsa AR, O'Brien AD.** 2000. Elastase in intestinal mucus enhances the cytotoxicity of Shiga toxin type 2d. J Biol Chem **275:**3713–3721. http://dx.doi.org/10.1074/jbc.275.5.3713.
14. **Bielaszewska M, Friedrich AW, Aldick T, Schurk-Bulgrin R, Karch H.** 2006. Shiga toxin activatable by intestinal mucus in Escherichia coli isolated from humans: predictor for a severe clinical outcome. Clin Infect Dis **43:**1160–1167. http://dx.doi.org/10.1086/508195.
15. **Bunger JC, Melton-Celsa AR, O'Brien AD.** 2013. Shiga toxin type 2dact displays increased binding to globotriaosylceramide in vitro and increased lethality in mice after activation by elastase. Toxins (Basel) **5:**2074–2092. http://dx.doi.org/10.3390/toxins5112074.
16. **Fuller CA, Pellino CA, Flagler MJ, Strasser JE, Weiss AA.** 2011. Shiga toxin subtypes display dramatic differences in potency. Infect Immun **79:**1329–1337. http://dx.doi.org/10.1128/IAI.01182-10.
17. **Siegler RL, Obrig TG, Pysher T, Tesh JVL, Denkers ND, Taylor FB.** 2003. Response to Shiga toxin 1 and 2 in a baboon model of hemolytic uremic syndrome. Pediatr Nephrol **18:**92–96.
18. **Stearns-Kurosawa DJ, Collins V, Freeman S, Tesh VL, Kurosawa S.** 2010. Distinct physiologic and inflammatory responses elicited in baboons after challenge with Shiga toxin type 1 or 2 from enterohemorrhagic *Escherichia coli*. Infect Immun **78:**2497–2504. http://dx.doi.org/10.1128/IAI.01435-09.
19. **Stearns-Kurosawa DJ, Collins V, Freeman S, Debord D, Nishikawa K, Oh SY, Leibowitz CS, Kurosawa S.** 2011. Rescue from lethal Shiga toxin 2-induced renal failure with a cell-permeable peptide. Pediatr Nephrol **26:**2031–2039. http://dx.doi.org/10.1007/s00467-011-1913-y.
20. **Endo Y, Tsurugi K, Yutsudo T, Takeda Y, Ogasawara T, Igarashi K.** 1988. Site of action of a Vero toxin (VT2) from Escherichia coli O157:H7 and of Shiga toxin on eukaryotic ribosomes. RNA *N*-glycosidase activity of the toxins. Eur J Biochem **171:**45–50.
21. **Saxena SK, O'Brien AD, Ackerman EJ.** 1989. Shiga toxin, Shiga-like toxin II variant, and ricin are all single-site RNA N-glycosidases of 28 S RNA when microinjected into *Xenopus* oocytes. J Biol Chem **264:**596–601.
22. **Karmali MA, Petric M, Lim C, Fleming PC, Arbus GS, Lior H.** 1985. The association between idiopathic hemolytic uremic syndrome and infection by verotoxin-producing *Escherichia coli*. J Infect Dis **151:**775–782. http://dx.doi.org/10.1093/infdis/151.5.775.
23. **Melton-Celsa AR, O'Brien AD.** 1998. Structure, biology, and relative toxicity of Shiga toxin family members for cells and animals, p 121–128. *In* Kaper JB, O'Brien AD (ed), *Escherichia coli* O157:H7 and other Shiga toxin-producing *E. coli* strains. ASM Press, Washington, DC.
24. **DeGrandis S, Law H, Brunton J, Gyles C, Lingwood CA.** 1989. Globotetraosylceramide is recognized by the pig edema disease toxin. J Biol Chem **264:**12520–12525.
25. **Ling H, Boodhoo A, Hazes B, Cummings MD, Armstrong GD, Brunton JL, Read RJ.** 1998. Structure of the Shiga-like toxin I B-pentamer complexed with an analogue of its receptor Gb3. Biochemistry **37:**1777–1788. http://dx.doi.org/10.1021/bi971806n.
26. **Fraser ME, Fujinaga M, Cherney MM, Melton-Celsa AR, Twiddy EM, O'Brien AD, James MN.** 2004. Structure of Shiga toxin type 2 (Stx2) from *Escherichia coli* O157:H7. J Biol Chem **279:**27511–27517. http://dx.doi.org/10.1074/jbc.M401939200.
27. **Kitov PI, Sadowska JM, Mulvey G, Armstrong GD, Ling H, Pannu NS, Read RJ, Bundle DR.** 2000. Shiga-like toxins are neutralized by tailored multivalent carbohydrate ligands. Nature **403:**669–672. http://dx.doi.org/10.1038/35001095.
28. **Paton AW, Morona R, Paton JC.** 2000. A new biological agent for treatment of Shiga toxigenic *Escherichia coli* infections and dysentery in humans. Nat Med **6:**265–270. http://dx.doi.org/10.1038/73111.
29. **Nishikawa K, Matsuoka K, Kita E, Okabe N, Mizuguchi M, Hino K, Miyazawa S, Yamasaki C, Aoki J, Takashima S, Yamakawa Y, Nishijima M, Terunuma D, Kuzuhara H, Natori Y.** 2002. A therapeutic agent with oriented carbohydrates for treatment of infections by Shiga toxin-producing *Escherichia coli* O157:H7. Proc Natl Acad Sci U S A **99:**7669–7674. http://dx.doi.org/10.1073/pnas.112058999.
30. **Mulvey GL, Marcato P, Kitov PI, Sadowska J, Bundle DR, Armstrong GD.** 2003. Assessment in mice of the therapeutic potential of tailored, multivalent Shiga toxin carbohydrate ligands. J Infect Dis **187:**640–649. http://dx.doi.org/10.1086/373996.
31. **Watanabe M, Matsuoka K, Kita E, Igai K, Higashi N, Miyagawa A, Watanabe T, Yanoshita R, Samejima Y, Terunuma D, Natori Y, Nishikawa K.** 2004. Oral therapeutic agents with highly clustered globotriose for treatment of Shiga toxigenic *Escherichia coli* infections. J Infect Dis **189:**360–368. http://dx.doi.org/10.1086/381124.
32. **Nishikawa K, Matsuoka K, Watanabe M, Igai K, Hino K, Terunuma D, Kuzuhara H, Natori Y.** 2005. Identification of the optimal structure for a Shiga toxin neutralizer with oriented carbohydrates to function in the circulation. J Infect Dis **191:**2097–2105. http://dx.doi.org/10.1086/430388.
33. **Nishikawa K.** 2011. Recent progress of Shiga toxin neutralizer for treatment of infections by Shiga toxin-producing Escherichia coli. Arch Immunol Ther Exp (Warsz) **59:**239–247. http://dx.doi.org/10.1007/s00005-011-0130-5.
34. **Nishikawa K, Watanabe M, Kita E, Igai K, Omata K, Yaffe MB, Natori Y.** 2006. A multivalent peptide-library approach identifies a novel Shiga toxin-inhibitor that induces aberrant cellular transport of the toxin. FASEB J **20:**2597–2599. http://dx.doi.org/10.1096/fj.06-6572fje.
35. **Watanabe-Takahashi M, Sato T, Dohi T, Noguchi N, Kano F, Murata M, Hamabata T, Natori Y, Nishikawa K.** 2010. An orally applicable Shiga toxin neutralizer functions in the intestine to inhibit the intracellular transport of the toxin. Infect Immun **78:**177–183. http://dx.doi.org/10.1128/IAI.01022-09.
36. **Tsutsuki K, Watanabe-Takahashi M, Takenaka Y, Kita E, Nishikawa K.** 2013. Identification of a peptide-based neutralizer that potently inhibits both Shiga toxins 1 and 2 by targeting specific receptor-binding regions. Infect Immun **81:**2133–2138. http://dx.doi.org/10.1128/IAI.01256-12.
37. **Kato M, Watanabe-Takahashi M, Shimizu E, Nishikawa K.** 2015. Identification of a wide range of motifs inhibitory to Shiga toxin by affinity-driven screening of customized divalent peptides synthesized on a membrane. Appl Environ Microbiol **81:**1092–1100. http://dx.doi.org/10.1128/AEM.03517-14.
38. **Ito H, Terai A, Kurazono H, Takeda Y, Nishibuchi M.** 1990. Cloning and nucleotide sequencing of Vero toxin 2 variant genes from Escherichia coli O91:H21 isolated from a patient with the hemolytic uremic syndrome. Microb Pathog **8:**47–60. http://dx.doi.org/10.1016/0882-4010(90)90007-D.
39. **Watanabe M, Igai K, Matsuoka K, Miyagawa A, Watanabe T, Yanoshita R, Samejima Y, Terunuma D, Natori Y, Nishikawa K.** 2006. Structural analysis of the interaction between Shiga toxin B-subunits and linear polymers bearing clustered globotriose residues. Infect Immun **74:**1984–1988. http://dx.doi.org/10.1128/IAI.74.3.1984-1988.2006.
40. **Lindgren SW, Samuel JE, Schmitt CK, O'Brien AD.** 1994. The specific activities of Shiga-like toxin type II (SLT-II) and SLT-II-related toxins of enterohemorrhagic *Escherichia coli* differ when measured by Vero cell cytotoxicity but not by mouse lethality. Infect Immun **62:**623–631.
41. **Oku Y, Yutsudo T, Hirayama T, O'Brien AD, Takeda Y.** 1989. Purification and some properties of a Vero toxin from a human strain of Escherichia coli that is immunologically related to Shiga-like toxin II (VT2). Microb Pathog **6:**113–122. http://dx.doi.org/10.1016/0882-4010(89)90014-4.
42. **Karve SS, Weiss AA.** 2014. Glycolipid binding preferences of Shiga toxin variants. PLoS One **9:**e101173. http://dx.doi.org/10.1371/journal.pone.0101173.

43. **O'Brien AD, Tesh VL, Donohue-Rolfe A, Jackson MP, Olsnes S, Sandvig K, Lindberg AA, Keusch GT.** 1992. Shiga toxin: biochemistry, genetics, mode of action, and role in pathogenesis. Curr Top Microbiol Immunol **180:**65–94.
44. **Persson S, Olsen KE, Ethelberg S, Scheutz F.** 2007. Subtyping method for *Escherichia coli* Shiga toxin (verocytotoxin) 2 variants and correlations to clinical manifestations. J Clin Microbiol **45:**2020–2024. http://dx.doi.org/10.1128/JCM.02591-06.
45. **Bunger JC, Melton-Celsa AR, Maynard EL, O'Brien AD.** 2015. Reduced toxicity of Shiga toxin (Stx) type 2c in mice compared to Stx2d is associated with instability of Stx2c holotoxin. Toxins (Basel) **7:**2306–2320. http://dx.doi.org/10.3390/toxins7062306.